SOLDIFICATION SEQUENCE OF Al-2,5wt.%Mg-0,7wt.%Li ALLOY

Franjo Kozina[1], Zdenka Zovko Brodarac[1], Primož Mrvar[2], Mitja Petrič[2]

[1]University of Zagreb Faculty of Metallurgy, Aleja narodnih heroja 3, 44103 Sisak, Croatia

[2]University of Ljubljana Faculty of Natural Sciences and Engineering, Aškarčeva 12, 1000 Ljubljana, Slovenia

Abstract

Determination of solidification sequence of Al-2,5wt.%Mg-0,7wt.%Li alloy represents a challenge due to the strong influence of chemical composition, grain structure and thermodynamic parameters on the phase precipitation and transformation. Modelling of equilibrium phase diagrams in correlation with simultaneous thermal analysis, X-ray diffraction and metallographic investigations enables determination of solidification sequence. Besides commonly precipitated intermetallic phases, expected in the alloy containing >2,0wt%Mg, stabile δ (AlLi) phase was also found. These phases nucleated at the α_{Al} grain boundaries and grow at the expense of previously precipitated metastable δ (Al_3Li) causing the formation of precipitation free zones.

***Keywords**: Al-2,5wt.%Mg-0,7wt.%Li alloy, lithium, magnesium, microstructure, solidification sequence*

1. INTRODUCTION

The interest in aluminium-magnesium-lithium (Al-Mg-Li) alloys is fuelled by several important considerations: density reduction, stiffness increase, enhanced corrosion resistance [1], fatigue crack grout resistance [2], and increase in fracture toughness, as well as the precipitation hardening [3]. Namely, every 1wt.% of Li addition provides approximately 3% decrease in density and 6% increase in Young's modulus [4] up to 4wt% [5]. Increasing the Li content above 1,3wt.% results in yield and tensile strength decrease [6], while the maximum strength is obtained in the range of 1,1-1,3wt.% of Li, respectively [7]. Lithium additions enable the formation of potent hardening precipitates [1], in particular δ' (Al_3Li) that are strongly influenced by chemical composition, grain structure and thermodynamic parameters [8]. This hardening precipitates can interact with dislocations therefore significantly increasing microstructural texture [9], as well as increase of sensitivity to long term low temperature exposure [4]. Solidification starts with α_{Al} dendritic network formation followed with eutectic reaction resulting in metastable δ' phase precipitation [10]. The similarities in the structure and lattice parameters of α_{Al} and δ' phase manifested with low coherency strains as well as low interfacial energy [11, 12, 13]. The other major phases nucleate heterogeneously on the grain boundaries [14] or dispersions present in solid solution of α_{Al} [15] and have a tendency to take over the δ' phase. Since Mg reduces solubility of Li in α_{Al}, the rest of solidification sequence is dictated by Li/Mg ratio. When Li/Mg ratio is high, peritectic reaction between α_{Al} and δ' phase leads to the formation of stabile δ (AlLi) precipitate. Even considering that the exact mechanisms of δ phase nucleation in respect to δ' is not completely clear [16], it grows due to the depletion of Li from bulked α_{Al} and therefore forming precipitation free zones (PFZ) [10]. PFZ contribute to the formation of cracks at the grain boundaries decreasing fatigue and corrosion resistance [4]. Increasing Mg content > 2,0wt.% increases the likelihood of ternary T (Al_2LiMg) phase formation. This incoherent equilibrium phase tends to precipitate at the high angle grain boundaries leading to the material softening and widening of the PFZ [17]. In both instances, high and low Li/Mg ratio, solidification sequence ends with precipitation of secondary eutectic Al_3Mg_2 on the grain boundaries of the last solidifying areas. Since it precipitate as a irregular coarse particle it cannot contribute to the strengthening effect [18].

2. EXPERIMENTAL

Determination of solidification sequence of Al-2,5wt.%Mg-0,7wt.%Li alloy has been done combining Computer aided thermodynamic diagram calculation (CALPHAD) under equilibrium conditions with differential scanning calorimetry (DSC) and microstructural analysis.

The alloy was prepared in an induction furnace under protective atmosphere of Ar and crucible cover. After Al block (technical purity) was melted, Mg was added. Li wrapped in Al-foil (commercial purity) was introduced using steel bell. Melt was stirred to ensure a homogenous distribution of Li, and cast into a steel mold without protective atmosphere, respectively. Chemical composition analysis was done using ARL™ 4460 Optical Mass Spectroscope.

Samples for metallographic analysis were prepared using grinding/polishing machine Pheonix Beta Biller SAD. The samples were echoed combining several etching solutions in order to observe grain boundaries and precipitates. While Olympus GX51 microscope was used to perform the optical microscopy, electron microscopy was done on Tescan, Vega TS 5136 MM equipped with energy dispersive spectrometer (EDS). Since EDS did not possess a possibility of light elements identification, exact predication of present phases has been done by XRD method using Philips PANalytical X'Pert PRO X-ray diffractometer.

A simultaneous thermal analysis using DSC method was performed applying heating and cooling rates of 2 K/min at Netzsch STA 409 C / CD. The temperatures significant for phase transformations and precipitation were identified and compared with those obtained by modeling.

3. RESULTS AND DISCUSSION

The chemical composition of Al-2,5wt.%Mg-0,7wt.%Li is given in Table 1.

Table 1 - The chemical compositions of Al-2,5wt.%Mg-0,7wt.%Li

Element, wt.%	Al	Li	Mg
Alloy	Bal.	0.726	2,480

A higher Mg content (>2,0wt.%Mg) ensuring low Li/Mg ratio indicates precipitation of ternary T phase at the expense of primary precipitated metastable δ' phase.

Modeling of Al-2,5wt.%Mg-0,7wt.%Li alloy using ThermoCalc (TCW 5.0) program resulted with equilibrium phase diagram revealing phase precipitations and transformations during solidification sequence (Figure 1).

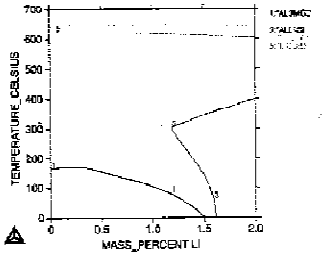

a)

Reaction	Temperature,°C
$L \rightarrow \alpha_{Al}$	622
$L+\alpha_{Al} \rightarrow \alpha_{Al}'+\delta$	368
$\alpha_{Al}'+\delta \rightarrow \alpha_{Al}''+Al_2LiMg$	257
$\alpha_{Al}'' \rightarrow \alpha_{Al}'''+Al_3Mg_2$	138

b)

Figure 1 - The Al-rich corner of Al-Mg-Li equilibrium phase diagram in respect to Li
a) Equlibrium phase diagram; b) Solidification sequence

According to equilibrium phase diagram, solidification sequence begins with α_{Al} dendritic network development. Lithium solubility decreases consequently causes the precipitation of stabile δ phase through peritectic reaction. Afterwards, δ phase reacts with Mg from bulked α_{Al}' and precipitates as T phase at the high angle grain boundaries. Irregular secondary Al_3Mg_2 eutectic precipitates at the last solidifying areas.

Significant temperatures of phase transformations and precipitations were established from heating and cooling curves using DSC method. Comparison of significant temperatures of phase transformation and precipitation with the results from XRD, solidification sequence in non-equilibrium conditions of Al-2,5wt.%Mg-0,7wt.%Li alloy was determined (Table 2).

Table 2 - Solidification sequence of Al-2,5wt.%Mg-0,7wt.%Li alloy in non-equilibrium conditions

Reaction	Temperature, °C	Description
$L \rightarrow \alpha_{Al}+\delta'$	620	Eutectic reaction of α_{Al} dendritic network development and precipitation of δ'
$\alpha_{Al}+\delta' \rightarrow \alpha_{Al}'+\delta$	605	Precipitation of stabile δ phase during peritectic reaction
$\alpha_{Al}'+\delta' \rightarrow \alpha_{Al}''+T$	492	Ternary T peritectic precipitation
$\alpha_{Al}'' \rightarrow \alpha_{Al}'''+Al_3Mg_2$	368	Secondary eutectic phase ending solidification sequence

Microstructure of Al-2,5wt.%Mg-0,7wt.%Li alloy was analyzed using optical and electron microscopy, while the individual phases were identified using literature etalons [4,10] (Figure 2.).

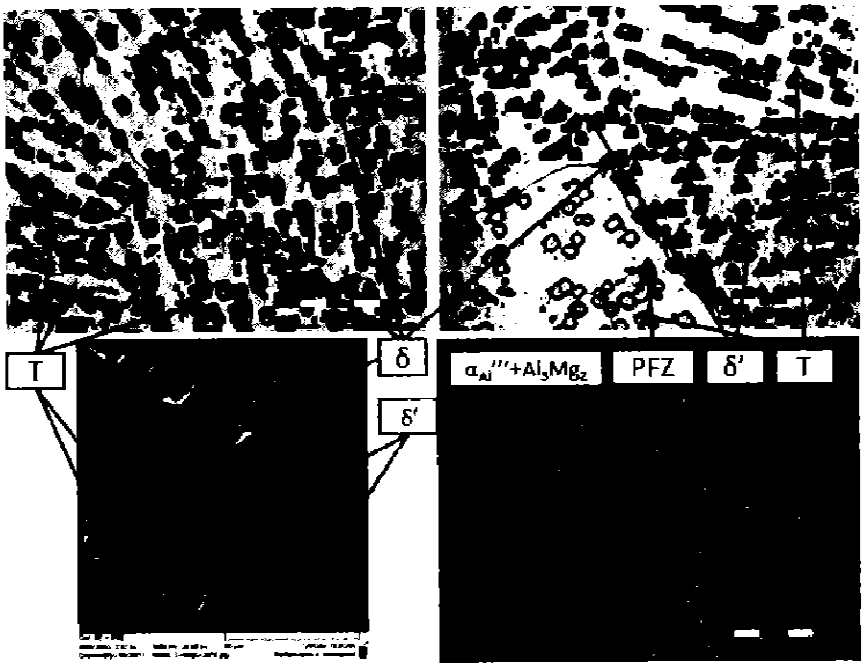

Figure 2 - Microstructural analysis of Al-2,5wt.%Mg-0,7wt.%Li

Due to the Li solubility decrese, aided by temperature decrease and Mg presence, metastable δ' phase will precipitate inside the grains simultaneously to α_{Al} dendritic network development. With the further temperature decrease, stabile δ will nucleate at the grain boundaries and grow due to the depletion of Li from previously developed α_{Al} and δ', leading to the formation of PFZ

(Figure 2). Elongated ternary T phase precipitates through peritectic reaction between Mg from bulk α_{Al}' and δ' phase. This phase will precipitate at the grain boundaries as well as inside the grain causing the decrease of precipitate number (Figure 2). Secondary eutectic reaction leads to the precipitation of Al_3Mg_2 decreasing Mg content in bulk α_{Al}'' and represents the end of the solidification sequence.

4. CONCLUSION

The Al-2,5wt.%Mg-0,7wt.%Li alloy investigation indicates the intensive influence of chemical composition and thermodynamic parameters correlation on the solidification sequence. Solidification starts with α_{Al} dendritic network development followed by eutectic reaction and metastable δ' phase precipitation. Despite of low Li/Mg ratio, Li solubility decrease causes precipitation of stabile δ phase. The rest of solidification is controlled by Mg from bulk α_{Al}. T phase precipitates in peritectic reaction between bulk α_{Al}' and δ' phase. Both, stabile δ phase and T phase nucleate at the grain boundaries of α_{Al} on the expense of precipitated metastable δ' phase causing the PFZ formation and widening. Solidification ends with secondary eutectic phase Al_3Mg_2.

ACKNOWLEDGEMENTS

This paper is supported by the funds of the University of Zagreb within the framework of Financial Support for Research "Design and Characterization of Innovative Engineering Alloys", Code: TP167.

REFERENCES

[1] R. J. Rioja, J. Liu, Metallurgical and Materials Transactions A., 43 A (2012) 3325-3337.
[2] C.J. Peel, B. Evans, D.S. McDarmaid, Material Research, 8 (3) (2005) 287-291.
[3] J. W. Martin, Aluminium-Lithium Alloys., Ann. Rev. Mater. Sci. 18 (1988) 101-119.
[4] R. J. Rioja, Material Science and Engineering. A 257 (1998) 100-107.
[5] K.K. Sankaran, N.J. Grant, Material Science and Engineering, 44 (2) (1980) p.213.
[6] R.K. Gupta, N. Nayan, G. Nagasireesha, S.C. Sharma, Material Science and Engineering A 420 (2006) 228-234.
[7] T.J. Lagan, J.R. Pickens, Proceedings of Fifth International Al-Li Chonference, March 27-31, Williamsburg, SAD, 1989, p.691.
[8] N.E. Prasad, S.V. Kamat, K.S. Prasad, G. Malakondaiah, V.V. Kutumbarao, Engineering Fracture Mechanic, 46 (2) (1993), 209-223.
[9] M. Trinca, A. Avalino, H. Germestani, J. Foyos, E.W. Lee, O.S. Es-Said, 331 (1) (2000) 3325-3337.
[10] N. Prasad, A. Eswera, A.Gokhale, R.J.H. Wanhill, Aluminium-Lithium Alloys, Aerospace Materials and Material Technologies, Butterworth-Heinemann, Oxford, 2013, p.67.
[11] A. Deschamps, C. Sigli, T. Mourey, F. de Geuser, W. Lefebvre, B. Davo, Acta Materialia 60 (2012) 1917-1928.
[12] B. Noble, S.E. Bray, Acta Materialia 40 (17) (1998) 6163-6171.
[13] B.C. Lee, J.K. Park, Acta Materialia 46 (12) (1998) 4181-4187.
[14] B. Noble, G.E. Thompson, Material Science Journal, 5 (1) (1971) 114-120.
[15] V.G. Davydov, L.B. Ber, E. Ya Kaputkin, V.I. Komov, O.G. Ukolova, E.A., Material Science and Engineering: A, 280 (1) (2000) 76-82.
[16] D.B. Williams, J.W. Edington, Metal Science, 9 (1) (2013) 529-532.
[17] A. Mogucheva, R. Kaibyshev, Metals, 6 (11) (2016) 545.
[18] Z.Z. Brodarac, F. Unkić, J. Medved, P. Mrvar, Kovove Materialy-Metallic Materials, 50 (1) (2012), 59-67.